

# Topological Properties of the Optical Operator Reconfiguration Network

Wang Xianchao<sup>1,3,\*</sup> and Zuo Kaizhong<sup>2,3</sup>

<sup>1</sup> School of Mathematics & Computational Science, Fuyang Normal College, Fuyang 236041, China

<sup>2</sup> School of Mathematics & Computer Science, Anhui Normal University, Wuhu 241000, China

<sup>3</sup> School of Computer Engineering and Science, Shanghai University, Shanghai 200072, China

Received: 15 Nov. 2014, Revised: 15 Feb. 2015, Accepted: 16 Feb. 2015

Published online: 1 Jul. 2015

**Abstract:** We present a first study on the reconfigurability of optical operators in the optical computing platform, ternary optical computer (TOC), from the viewpoint of complex network. In the optical operator reconfiguration network (OORN), vertexes stand for the basic operating units (BOUs) and the optical operators, and directed edges indicate the dynamic reconfiguration relations between BOUs and operators. We find that the OORN has small-world pattern and scale-free feature as other complex networks. In order to describe the clustering property of the OORN, we propose an approach for characterizing the OORN by introducing a new numerical feature, density of vertex. Its density distribution follows power-law distribution as its cumulative degree distribution. In addition, we find that it is reasonable and optimal to use 50 kinds of BOUs in real TOC system by comparing the OORNs with different kinds of BOUs.

**Keywords:** Ternary optical computer, optical operator reconfiguration network, basic operating unit, density

## 1 Introduction

The solution to the Königsberg bridge problem by the Swiss mathematician Leonhard Euler started the method to describe the objective world by use of network. Large and complex stochastic networks are conspicuous in science and everyday life, and have attracted a great deal of interest. In these networks, the individuals or organizations are looked upon as nodes and their relationships as edges. If the edges are directed in a network, it is called directed one. Otherwise, it is called undirected one.

Biological [1,2,3,4,5,6,7] and chemical systems [8,9], neural networks [10,11], social interacting species [12,13,14], the Internet [15], the World Wide Web [16], transportation systems [17,18,19], communication networks [20,21,22], natural language [23,24,25] and disease transmission networks [26,27,28] are only a few examples of complex systems composed by a large number of highly interconnected units. Obviously, the communication networks and disease transmission networks are directed. People have found that there are some features, such as small-world property [1,3,4,15,

21,29,30] and scale-free nature [10,21,30,31] in these real networks. In recent years, some dynamic reconfiguration networks have attracted some researchers' attentions [2,3,10,11,32]. In this paper, we'll study another dynamic reconfiguration network and its topological properties.

On the other hand, Jin et al. proposed the principle and architecture of a ternary optical computer(TOC) [33,34]. Many achievements have been obtained in the past one decade, especially in recent years. For instance, the decrease radix design principle(DRDP) [35], which discussed how to build the configurable optical processor, was proposed. And a TOC experimental platform was built according to the principle. Based on MSD number system, the optical three-step addition and optical vector-matrix multiplication [36] were performed on the experimental platform. Meanwhile, the principle of adder in the TOC was proposed [37]. A one-step MSD optical adder, which improved the computation speed of the TOC in some degree, was designed and implemented [38]. A novel TOC experimental platform [39] was built in 2011, according to the DRDP. It had some good features. For example, it had high computation accuracy for it was

\* Corresponding author e-mail: [wxcdx@126.com](mailto:wxcdx@126.com)

digital; it had computation flexibility for it could reconfigure dynamically optical processor according to user requirement; it had high computation speed for the MSD adder was carry-free and the TOC was a multiple-instruction multiple-data system [39]. In order to make better use of these features and manage efficiently these optical operators, we will focus on the optical operator reconfiguration network(OORN) and their principal topological properties.

This paper is organized as follows. Section 2 briefs the related work, including the DRDP and principal properties of complex networks. Section 3 presents the reconfigurability of optical operators in the TOC from the viewpoint of complex networks. In the OORN, nodes stand for the basic operating units (BOUs) and the optical operators, and directed edges indicate the dynamic reconfiguration relations between BOUs and operators. Section 4 focuses on studying the key topological properties of the OORN. The results show that the OORN is scale-free, small-world, and so on. At the same time, in order to adequately describe the OORN, it presents a novel idea, density and density distribution. In addition, it compares the OORNs with different numbers of BOUs. Section 5 illustrates the concluding remarks and the consideration of future work.

## 2 Related work

In this section we discuss the related work, including the DRDP and principal properties of complex networks.

### 2.1 Decrease radix design principle

Obviously, among these achievements about the TOC, the most important one is the DRDP. According to it, any of the  $n^{n^2}$  two-input  $n$ -valued logic operations can be implemented by combination of some BOUs. And to  $n$ -valued logic, there are  $n^2(n-1)$  different BOUs. The implementation of an operation by composing some BOUs is called reconfiguration[35].

If  $n = 3$ , it can be easily seen that there are altogether 19,683 kinds of two-input tri-valued logic operations and 18 kinds of the most fundamental BOUs. To make full use of the TOC hardware, these fundamental BOUs can be merged functionally according to some rules. After being merged, there are 50 kinds of BOUs altogether[39]. For convenience, these BOUs are numbered, the BOU with No.  $p$  written as  $\text{BOU}_p$ , the BOUs with No. from  $p$  to  $q$  as  $\text{BOU}_{p-q}$ , and the BOUs with No.  $p$  and  $q$  as  $\text{BOU}_{p,q}$ . After being numbered,  $\text{BOU}_{1-18}$  are the most fundamental BOUs. Meantime, each of  $\text{BOU}_{21-44}$  and  $\text{BOU}_{51-58}$  is merged functionally by two and three of  $\text{BOU}_{1-16}$ , respectively. For example,  $\text{BOU}_{21}$  is merged by  $\text{BOU}_1$  and  $\text{BOU}_3$ , and  $\text{BOU}_{51}$  by  $\text{BOU}_1$ ,  $\text{BOU}_3$  and  $\text{BOU}_5$ [39]. Nonetheless, all of the BOUs are the same in

hardware structure, shown in FIG. 1. In the structure, a liquid crystal cell (LCC) was sandwiched by two pieces of polarizer, P1 and P2. A nonenergized LCC could twist the polarized light entering it by  $90^\circ$  on exit and an electric field applied across the LCC could make the polarized light go through without being twisted. Moreover, P1 and P2 could be a piece of horizontal or vertical polarizer.

Aggregating all the BOUs with the same polarizers, we set up the optical operators of the TOC at Shanghai University in 2011. Obviously, these operators were made up of four parts, called VV, VH, HH and HV, respectively. Each part had  $24 \times 24$  pixels i.e. 576 BOUs and an experimental system was designed and implemented to manage these operators [39]. Based on the DRDP, the system was also a dynamically reconfigurable optical computing platform. In other words, any one-bit two-input tri-valued logic processor could be dynamically reconfigured at runtime by no more than 6 BOUs in total, and no more than 3 BOUs were needed in each part.

### 2.2 Principal properties of complex networks

In this subsection, we describe some significant topological properties, such as average path length, degree distribution, clustering coefficient [29,40], which appear to be common to real networks of many different types.

The path length  $d_{ij}$  is the number of the edges or the length of the geodesic on the shortest path from node  $i$  to node  $j$  in real networks. And the average path length  $L$  of a network can be obtained according to the following formula:

$$L = \frac{1}{\frac{1}{2}n(n-1)} \sum_{i < j} d_{ij}, \quad (1)$$

where  $n$  is the number of the nodes. In most real networks,  $L$  is far less than  $n$ . The property is called small-world pattern [19,40,41,42,43,44,45,46].

The degree  $k_i$  of node  $i$  is the number of edges connected to it. Average degree  $\bar{k}$  of a network is the mean of degrees over all of the nodes. And  $p(k)$  is the probability that a node chosen uniformly at random has

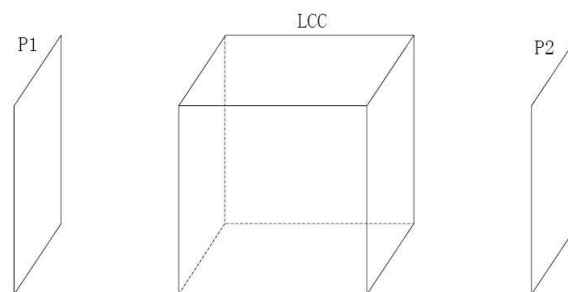


Fig. 1: Structure of a BOU.

degree  $k$ . Thus, the degree distribution of a network can be presented with  $p(k)$ . An alternative way of presenting degree data is to use the cumulative degree function

$$P(k) = \sum_{k'=k}^{\infty} p(k'). \tag{2}$$

It can describe the real networks which have great degree nodes. In most of real networks,  $P(k)$  follows power-law distributions, that is,  $P(k) \sim k^{-\gamma}, \gamma > 0$ . Networks with power-law degree distributions are referred to as scale-free networks [16,22,45,46].

Clustering coefficient  $C$  describes the clustering level of nodes in a network [19,29,31,40,43]. The way of calculating the clustering coefficient  $C_i$  of node  $i$  is as follows:

$$C_i = \frac{\Delta_i}{\Lambda_i}, \tag{3}$$

where  $\Delta_i$  and  $\Lambda_i$  are the numbers of triangles and transitive triples connected to node  $i$ , respectively. Obviously, the number of the former is less than or equal to the one of the latter. In other words,  $0 \leq C_i \leq 1$ . The clustering coefficient  $C$  of a network is defined as the mean of clustering coefficients over all nodes. That is to say,

$$C = \frac{1}{n} \sum_i C_i. \tag{4}$$

These properties are foundation to study many real networks. Besides them, there are some other properties, such as degree correlation [21], network resilience, community structure [47] and mixing pattern [40].

### 3 Optical operator reconfiguration network in the ternary optical computer

As mentioned above, any two-input tri-valued logic operation can be implemented by use of 50 kinds of BOUs. At the same time, there are three stable light states, no-intensity light, horizontally polarized light and vertically polarized light, to present information in the TOC. In order to achieve these logic operations, they must be firstly mapped into the 8311 kinds of physical operators which can be reconfigured with the 50 kinds of BOUs. There are still 8310 kinds of physical operators except for the operator whose optical states are all no-intensity light. These physical operators, including 50 kinds of BOUs, are numbered from 1 to 8310 to distinguish them. Thus, each BOU has two Nos.. For example, the operator No. of the BOU<sub>25</sub> is 2227. However, for each BOU, we don't use its operator No. but its BOU No..

The first approach to capture the global properties of a complex system is to model it as a network where nodes represent the dynamic units, and edges stand for the interactions between nodes. Therefore, to research the

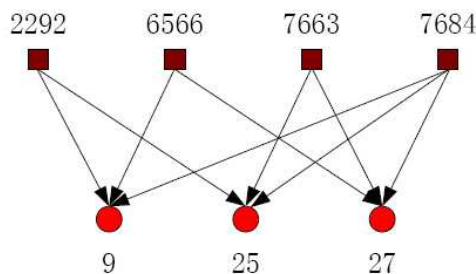


Fig. 2: Topology of the optical operator reconfiguration network composed by operators and BOUs in Table 1.

topological properties of the optical operator reconfiguration network in the TOC, we also model it as a network where nodes represent optical operators and BOUs, and directed edges stand for the reconfigurable relations between them. For instance, we consider a simple optical operator reconfiguration network. In this network, we investigate the operators with No. 2292, 6566, 7663 and 7684. The BOU usage of these operators is shown in Table 1, where the digits stand for the Nos. of operators and BOUs. In other words, the table shows the reconfiguration relations between these optical operators and BOU<sub>9,25,27</sub>. For example, the operator with No.2292 is dynamically reconfigured with the BOU<sub>9,25</sub>.

Fig. 2 illustrates a simple optical operator reconfiguration network according to the reconfiguration information in Table 1. Here the directed edges stand for the reconfiguration relations with which the operators can be dynamically reconfigured by different BOUs. Obviously, square and circle nodes stand for operators and BOUs, respectively.

There are some distinct features in the optical operator reconfiguration network as follows:

- ◆1) There is no edge between BOU nodes or between operator nodes. In other words, it is a bipartite graph.
- ◆2) It is directed.
- ◆3) There is no node whose degree is 0 or 1 in the network.

In order to study the topological properties of OORN, we must construct the OORN with all physical operators and BOUs. Fig. 3 illustrates the OORN with all operators and BOUs. Here circles stand for BOU nodes and squares for operator nodes, and the directed edges similarly stand

Table 1: Operators and BOUs to reconfigure a simple optical operator reconfiguration network.

Operators	BOUs		
2292	9	25	
6566	9	27	
7663	25	27	
7684	9	25	27

for the reconfiguration relations between operators and BOUs. It can be easily seen that the operator nodes have small out-degrees and the BOU nodes have terribly great in-degrees. To obtain the in-degree of each BOU node, we firstly count each BOU usage, shown in Table 2. Where 'Frequency' means the times of each BOU when 8310 kinds of optical operators are reconfigured dynamically with different BOUs. For example, it is 707 times for BOU<sub>2</sub> to reconfigure different optical operators.

At the same time, in Table 2, the frequency of each BOU includes the time it uses itself. In other words, the digits, decreased by one, in the second and the fourth columns are the in-degrees of relevant BOUs in the OORN. For example, the in-degree of BOU<sub>2</sub> is 706.

On the other hand, we also count the numbers of optical operators which can be reconfigured dynamically with different numbers of BOUs, shown in Table 3. For example, there are 652 optical operators which can be reconfigured dynamically with 2 BOUs.

As mentioned above, there is no node whose degree is 0 or 1. Therefore, except for the first row, the digits in the first column of Table 3 are the out-degrees of operator nodes and the digits in the second column are the numbers of operator nodes with relevant out-degrees. For example, the second row illustrates that there are 652 operator nodes with out-degree 2 in the OORN with all physical operators and BOUs.

**Table 2:** BOU usage in the OORN with all operators and BOUs.

No.	Frequency	No.	Frequency
1	707	28	400
2	707	29	400
3	809	30	262
4	809	31	400
5	1309	32	268
6	1309	33	274
7	815	34	400
8	815	35	280
9	917	36	160
10	917	37	280
11	1429	38	268
12	1429	39	274
13	1441	40	400
14	1441	41	280
15	1561	42	160
16	1561	43	280
17	2187	44	268
18	2187	51	78
21	394	52	78
22	400	53	78
23	400	54	78
24	262	55	78
25	400	56	78
26	268	57	78
27	394	58	78

According to Table 2 and Table 3, we can obtain the node degree information, shown in Table 4, of the OORN. In the table, we don't distinguish out-degree and in-degree.

## 4 Topological properties of the optical operator reconfiguration network

In this section, we discuss some principal topological properties of the OORN modeled with all physical operators and BOUs.

### 4.1 Density distribution

As mentioned above, there is no edge to connect any two BOU nodes or any two operator nodes in the OORN. In other words, for each node  $i$ ,  $\Delta_i$  is equal to zero. Therefore, according to Eq. (3), its clustering coefficient  $C_i$  is zero, and the clustering coefficient  $C$  of the OORN is also zero, according to Eq. (4). Thus, clustering coefficient can't adequately describe the clustering property of the OORN.

In order to better describe the clustering property of the OORN, we propose an idea of the density. Density  $D_i$  of node  $i$  represents the clustering level of the edges which are connected to it. In other words,  $D_i$  is involved with not only the degree  $k_i$  of node  $i$  but also the number of the edges between its adjacent nodes. The way of

**Table 3:** Number of operators which are reconfigured with different numbers of BOUs in the OORN with all operators and BOUs.

Number of BOUs	Number of operators
1	50
2	652
3	2674
4	3584
5	1266
6	84

**Table 4:** Degree information of the OORN with all operators and BOUs.

Degree	Number of nodes	Degree	Number of nodes
2	652	814	2
3	2674	808	2
4	3584	706	2
5	1266	399	8
6	84	393	2
2186	2	279	4
1560	2	273	2
1440	2	267	4
1428	2	261	2
1308	2	159	2
916	2	77	8

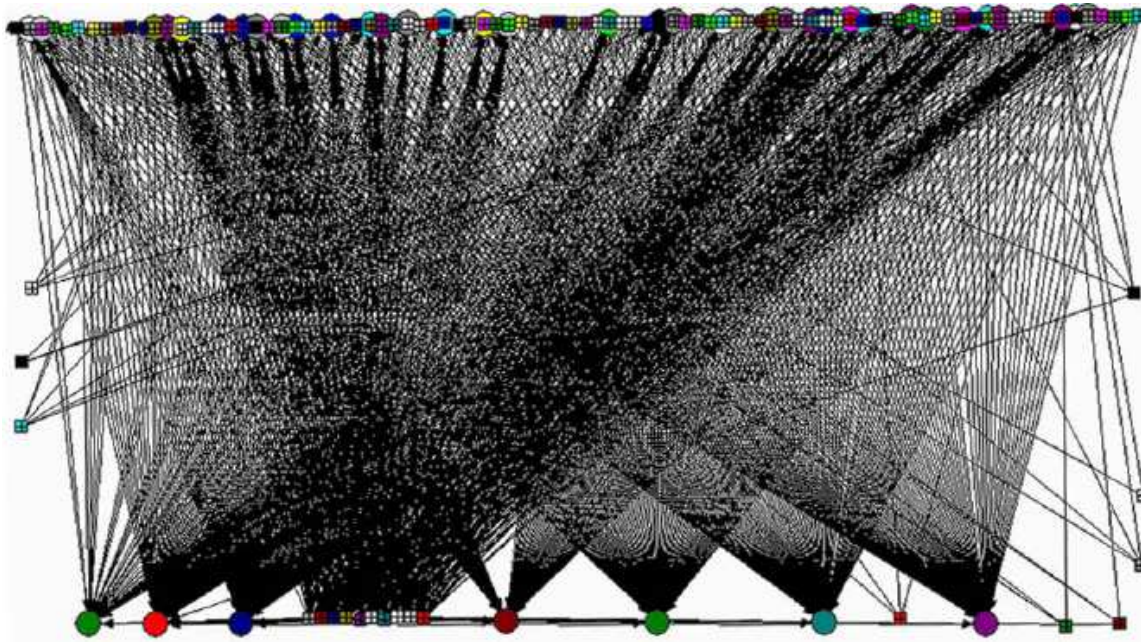


Fig. 3: OORN with all operators and BOUs.

calculating  $D_i$  is similar to the one of calculating  $C_i$ . Supposing that there are  $k_i$  nodes connected to the node  $i$ , the way of calculating  $D_i$  is shown in Eq. (5):

$$D_i = \frac{E_i}{\frac{k_i(k_i+1)}{2}}, \tag{5}$$

where  $k_i(k_i + 1)/2$  represents the number of all possible edges between the  $k_i + 1$  nodes, and  $E_i$  stands for the actual edges between them. Obviously, if the degree  $k_i$  of node  $i$  is equal to 1, its  $D_i$  is 1. Similarly, there is a regulation that  $D_i$  is 0 if  $k_i$  is equal to 0. The density  $D(k_i)$  is defined as the mean of densities over all nodes with degree  $k_i$  in a network, and the density  $D$  as the mean of densities over all nodes.

In bipartite network,  $E_i$  is equal to the degree  $k_i$  of node  $i$  since there is no edge between  $k_i$  BOU nodes or between operator nodes. Thus, Eq. (5) is changed into Eq. (6):

$$D_i = \frac{2}{(k_i + 1)}. \tag{6}$$

According to the formula, it can be easily seen that the density  $D_i$  of each BOU node in Fig. 2 is 0.5 since its degree  $k_i$  is equal to 3. However, the clustering coefficient  $C_i$  of each node in Fig. 2 is zero.

After each  $D(k_i)$  being calculated, the density  $D(k_i)$  distribution of the OORN with all physical operators and BOUs is shown in Fig. 4. Here the horizontal axis for each panel denotes vertex degree  $k_i$  (in-degrees for BOUs and out-degrees for operators) and the vertical axis indicates density  $D(k_i)$ . At the same time, Fig. 4(a) is

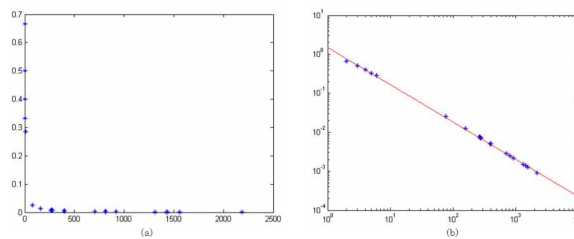
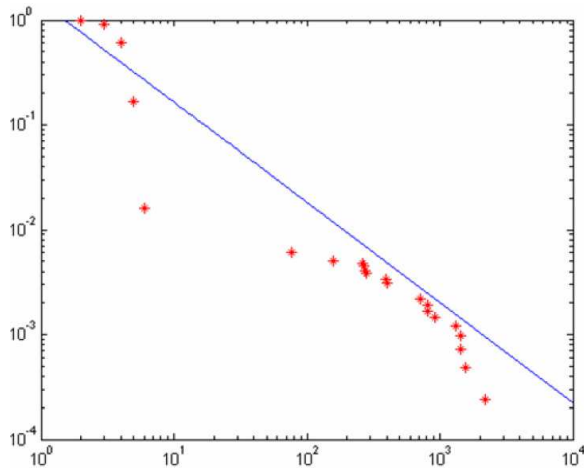


Fig. 4: Density  $D(k_i)$  distribution of the OORN with all operators and BOUs.

shown on normal scales and Fig. 4(b) shown on logarithmic scales. The line in Fig. 4(b) is the nonlinear regression of density  $D(k_i)$ . In addition, its equation is  $y = 1.4936x^{0.955}$ , and their linear correlation coefficient is 0.9995. In Fig. 4(a), it can be seen that the  $D(k_i)$  follows power-law distribution. Moreover, according to the  $D_i$  of each node, we can easily obtain the density  $D$ , which is equal to 0.4394, of the OORN.

### 4.2 Other important properties

In order to investigate other important properties of the OORN, it is looked upon as an undirected network. Thus, the average path length  $L$  is equal to 27.2537. It can be easily found that  $L$  is terribly less than the number of nodes, 8310, in the OORN with all physical operators and BOUs. In other words, the OORN has the small-world property.



**Fig. 5:** Cumulative degree  $P(k)$  distribution for the OORN in the TOC system.

Meanwhile, the average degree  $\bar{k}$ , obtained according to Table 4, is 3.6698. Obviously, the clustering coefficient of each node in the OORN is zero and its clustering coefficient  $C$  is zero. And Fig. 5 shows the cumulative degree distribution  $P(k)$  on logarithmic scales. Here the horizontal axis is vertex degree  $k_i$  and the vertical axis is the cumulative probability distribution of degrees, i.e., the fraction of vertices that have degree greater than or equal to  $k_i$ . And the line is the nonlinear regression of cumulative degree  $P(k)$ . Moreover, its equation is  $y = 1.0296x^{0.9921}$ , and their linear correlation coefficient is 0.9171. It can be seen that the cumulative degrees approximately follow power-law distribution. Therefore, the OORN with all physical operators and BOUs is nearly scale-free.

### 4.3 Comparison of the optical operator reconfiguration network with various kinds of BOUs

As mentioned above, the most fundamental BOUs can be emerged functionally to generate other kinds of BOUs,  $BOU_{21-44}$  and  $BOU_{51-58}$ . Thus, the dynamic reconfiguration of operators can be based on various BOUs, such as 18 kinds of the most fundamental BOUs, 26 kinds of BOUs (including  $BOU_{1-18}$  and  $BOU_{51-58}$ ), 42 kinds of BOUs (including  $BOU_{1-18}$  and  $BOU_{21-44}$ ) and 50 kinds of BOUs (including  $BOU_{1-18}$ ,  $BOU_{21-44}$  and  $BOU_{51-58}$ ). Therefore, different OORNs with various BOUs can be constructed.

Table 5 shows the comparison of the OORNs with various BOUs. Where 'BOU' is the kinds of BOUs which are used to construct the OORNs, and 'Operator', 'Edge', 'C', 'D', 'L', and ' $\bar{k}$ ' are the number of physical operators(including BOUs), the number of edges,

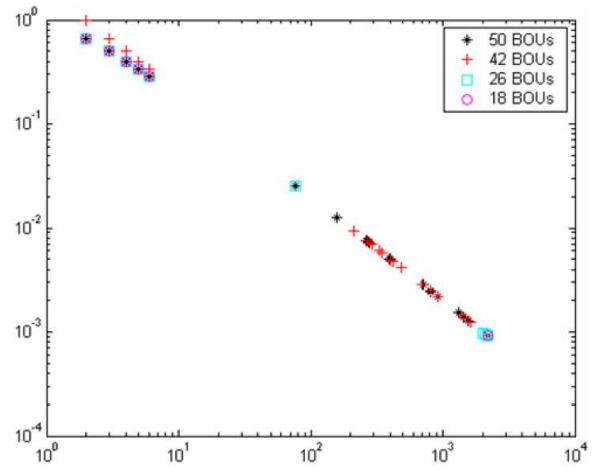


**Fig. 6:** Density  $D(k_i)$  distributions for the OORNs with various BOUs.

clustering coefficient, density, average path length, average degree of the OORNs, respectively.

From Table 5, we can see that there are the same number of optical operators and the clustering coefficients of these OORNs are all zero. At the same time, the densities and average path lengths increase and average degrees decrease with the increase of the number of BOUs. The reason is that the number of nodes is unchangeable while the number of edges decreases with the increase of the number of BOUs.

On the other hand, the number of operators provided by the TOC is unchangeable in real application. Therefore, the TOC can provide more data-bits, and process more data in parallel if more kinds of BOUs are used in real system. In other words, if density  $D$  and average path length  $L$  are greater and average degree  $\bar{k}$  is smaller, the chosen BOUs can make better use of the parallelism of the TOC. However, there are up to 50 kinds of BOUs to use in the TOC system. Consequently, it is reasonable and optimal to use 50 kinds of BOUs in real TOC system. Fig. 6 shows the density  $D(k_i)$  distributions for the OORNs with various kinds of BOUs. Similarly, the horizontal axis is vertex degree  $k_i$  and the vertical axis is density  $D(k_i)$ . And they are both shown on logarithmic scales. It can be seen that their density distributions all follow power-law distribution, regardless of the kinds of BOUs used in the TOC system.

**Table 5:** Comparison of different OORNs with various BOUs.

BOU	Operator	Edge	C	D	L	$\bar{k}$
18	8310	39348	0	0.358	18.855	4.735
26	8310	38092	0	0.371	20.046	4.584
42	8310	31032	0	0.433	26.745	3.734
50	8310	30496	0	0.439	27.254	3.670

## 5 Conclusions

In this paper, we have investigated the reconfigurability of optical operators in the TOC from the viewpoint of complex networks. With the help of complex networks, we have obtained some important and interesting topological characteristics of the optical operator reconfiguration network, such as average path length, clustering coefficient, average degree and degree distribution. These numerical results have shown that the OORN simultaneously exhibits small-world effect and scale-free degree distribution, and clustering coefficient can't adequately show the features of the networks. In addition, we have proposed a novel method, density of node, to illustrate the features of the networks, studied their density distributions, and found that both its density distribution and degree distribution follow power-law distribution.

Moreover, we have compared the optical operator reconfiguration network with various kinds of BOUs. On the basis of the comparison, we have drawn a conclusion that it is reasonable and optimal to use 50 kinds of BOUs in real TOC system. To some degree, the conclusion provides theoretical foundation for selecting the kinds of BOUs in the TOC system. In the future, we will continue investigating the other topological properties, such as network resilience, degree correlation, community structure and mixing pattern.

## Acknowledgments

This work was supported by the National Natural Science Foundation of China (NSFC) (No. 61073049, 61103054), the National Special Major of China (No. TS11496), Comprehensive Reform Pilot Project of Anhui Province (No. 2013zy167), and Comprehensive Reform Pilot Project of Fuyang Normal College (No. 2013ZYSD05). The authors were grateful to Yi Jin for providing the optical platform and giving some good advice on the paper. And the authors also would like to thank the reviewers for their helpful comments, remarks, and suggestions, which led to improvements of the paper.

## References

- [1] O. Sporns, C.J Honey, Small worlds inside big brains, Proceedings of the National Academy of Sciences of the United States of America **103**, 19219-19220 (2006).
- [2] D.S Bassett, N.F Wymbs, M.A Porter, P.J Mucha, J.M Carlson, S.T Grafton, Dynamic reconfiguration of human brain networks during learning, Proceedings of the National Academy of Sciences of the United States of America **108**, 7641-7646 (2011).
- [3] D.S Bassett, A. Meyer-Lindenberg, S. Achard, T. Duke, E. Bullmore, Adaptive reconfiguration of fractal small-world human brain functional networks, Proceedings of the National Academy of Sciences of the United States of America **103**, 19518-19523 (2006).
- [4] D.S Goldberg, F.P Roth, Assessing experimentally derived interactions in a small world, Proceedings of the National Academy of Sciences of the United States of America **100**, 4372-4376 (2003).
- [5] H. Jeong, B. Tombor, R. Albert, Z.N Oltvai, A.-L Barabási, The large-scale organization of metabolic networks, Nature **407**, 651-654 (2000).
- [6] P. Uetz, L. Giot, G. Cagney, et al, A comprehensive analysis of protein-protein interactions in *saccharomyces cerevisiae*, Nature **403**, 623-627 (2000).
- [7] A. Sethia, J. Eargleb, A.A Blacka, Z. Luthey-Schulten, Dynamical networks in tRNA:protein complexes, Proceedings of the National Academy of Sciences of the United States of America **106**, 6620-6625 (2009).
- [8] C. Conradi, D. Flockerzi, J. Raisch, J. Stelling, Subnetwork analysis reveals dynamic features of complex (bio)chemical networks, Proceedings of the National Academy of Sciences of the United States of America **104**, 19175-19180 (2007).
- [9] T. Scholak, Fernando de Melo, T. Wellens, F. Mintert, A. Buchleitner, Efficient and coherent excitation transfer across disordered molecular networks, Physical Review E **83**, 021912 (2011).
- [10] G. Grinstein, R. Linsker, Synchronous neural activity in scale-free network models versus random network models, Proceedings of the National Academy of Sciences of the United States of America **102**, 9948-9953 (2005).
- [11] M. Zhao, C.S Zhou, Y.H Chen, B. Hu, B.H Wang, Complexity versus modularity and heterogeneity in oscillatory networks: Combining segregation and integration in neural systems, Physical Review E **82**, 046225 (2010).
- [12] A. Montanaria, A. Saberi, The spread of innovations in social networks, Proceedings of the National Academy of Sciences of the United States of America **107**, 20196-20201 (2010).
- [13] Z.-K Zhang and C. Liu, A hypergraph model of social tagging networks, Journal of Statistical Mechanics: Theory and Experiment **2010**, P10005, 2010.
- [14] Z.K Zhang, C. Liu, A hypergraph model of social tagging networks, J. Stat. Mech. P10005 (2010).
- [15] D. Liben-Nowell, J. Kleinberg, Tracing information flow on a global scale using Internet chain-letter data, Proceedings of the National Academy of Sciences of the United States of America **105**, 4633-4638 (2008).
- [16] A.-L Barabási, R. Albert, H. Jeong, Scale-free characteristics of random networks: The topology of the World Wide Web, Physica A: Statistical Mechanics and its Applications **281**, 69-77 (2000).
- [17] R. Guimera, S. Mossa, A. Turtleschi, L.A.N Amaral, The worldwide air transportation network: Anomalous centrality, community structure, and cities' global roles, Proceedings of the National Academy of Sciences of the United States of America **102**, 7794-7799 (2005).
- [18] J. Zhang, X.B Cao, W.B Du, K.Q Cai, Evolution of Chinese airport network, Physica A: Statistical Mechanics and its Applications **389**, 3922-3931 (2010).
- [19] K.A Seaton, L.M Hackett, Stations, trains and small-world networks, Physica A: Statistical Mechanics and its Applications **339**, 635-644 (2004).

- [20] H. Ebel, L.-I Mielsch, S. Bornholdt, Scale-free topology of e-mail networks, *Physical Review E* **66**, 035103 (2002).
- [21] Y.C Zhang, Z.Z Zhang, S.G Zhou, J.H Guan, Deterministic weighted scale-free small-world networks, *Physica A: Statistical Mechanics and its Applications* **389**, 3316-3324 (2010).
- [22] S. Uddin, S.T.H Murshed, L. Hossain, Power-law behavior in complex organizational communication networks during crisis, *Physica A: Statistical Mechanics and its Applications* **390**, 2845-2853 (2011).
- [23] S.G Zhou, G.B Hu, Z.Z Zhang, J.H Guan, An empirical study of Chinese language networks, *Physica A: Statistical Mechanics and its Applications* **387**, 3039-3047 (2008).
- [24] L. Sheng, C.G Li, English and Chinese languages as weighted complex networks, *Physica A: Statistical Mechanics and its Applications* **388**, 2561-2570 (2009).
- [25] S.Y Yu, H.T Liu, C.S Xu, Statistical properties of Chinese phonemic networks, *Physica A: Statistical Mechanics and its Applications* **390**, 1370-1380 (2011).
- [26] S. Meloni, A. Arenas, Y. Moreno, Traffic-driven epidemic spreading in finite-size scale-free networks, *Proceedings of the National Academy of Sciences of the United States of America* **106**, 16897-16902 (2009).
- [27] R. Durrett, Some features of the spread of epidemics and information on a random graph, *Proceedings of the National Academy of Sciences of the United States of America* **107**, 4491-4498 (2010).
- [28] M. Salathé, M. Kazandjieva, J.W Lee, P. Levis, M.W Feldman, J.H Jones, A high-resolution human contact network for infectious disease transmission, *Proceedings of the National Academy of Sciences of the United States of America* **107**, 22020-22025 (2010).
- [29] S. Boccaletti, V. Latora, Y. Moreno, M. Chavez, D.-U Hwang, Complex networks: Structure and dynamics, *Physics Reports* **424**, 175-308 (2006).
- [30] Q. Guo, T. Zhou, J.G Liu, W.J Bai, B.H Wang, M. Zhao, Growing scale-free small-world networks with tunable assortative coefficient, *Physica A: Statistical Mechanics and its Applications* **371**, 814-822 (2006).
- [31] A.A Tsonis, K.L Swanson, G.L Wang, Estimating the clustering coefficient in scale-free networks on lattices with local spatial correlation structure, *Physica A: Statistical Mechanics and its Applications* **387**, 5287-5294 (2008).
- [32] L.Y Lü, T. Zhou, Link prediction in complex networks: A survey, *Physica A: Statistical Mechanics and its Applications* **390**, 1150-1170 (2011).
- [33] Y. Jin, H.C He, Y.T Lü, Ternary optical computer principle, *Science in China Series F* **46**, 145-150 (2003).
- [34] Y. Jin, H.C He, Y.T Lü, Ternary Optical Computer Architecture, *Physical Scripta* **T118**, 98-101 (2005).
- [35] J. Y. Yan, Y. Jin, K. Z. Zuo, Decrease-radix design principle for carrying/borrowing free multi-valued and application in ternary optical computer, *Sci. China Ser. F* **51**, 1415-1426 (2008).
- [36] X.C Wang, J.J Peng, M. Li, Z.Y Shen, S. Ouyang, array-free vector-matrix multiplication on a dynamically reconfigurable optical platform, *Applied Optics* **49**, 2352-2362 (2010).
- [37] Y. Jin, Y.F Shen, J.J Peng, S.Y Xu, G.T Ding, D.J Yue, H.H You, Principles and construction of MSD adder in ternary optical computer, *Science China Information Sciences* **53**, 2159-2168 (2010).
- [38] K. Song and Y.P Liu, Design and implementation of the one-step msd adder of optical computer, *Applied Optics* **51**, 917C926 (2012).
- [39] X.C Wang, J.J Peng, S. Ouyang, Control method for the optical components of a dynamically reconfigurable optical platform, *Applied Optics* **50**, 662-670 (2011).
- [40] M.E.J Newman, The structure and function of complex networks, *SIAM Review* **45**, 167-256 (2003).
- [41] S. Milgram, The small world problem, *Psychology Today* **1**, 61-67 (1967).
- [42] D.J Watts, S.H Strogatz, Collective dynamics of 'small-world' networks, *Nature* **393**, 440-442 (1998).
- [43] W. Y Li, Y. J. Lin, Y. Liu, The structure of weighted small-world networks, *Physica A: Statistical Mechanics and its Applications* **376**, 708-718 (2007).
- [44] S. Schettler, A structured overview of 50 years of small-world research, *Social Networks* **31**, 165-178 (2009).
- [45] J.H Guan, Y.W Wu, Z.Z Zhang, S.G Zhou, Y.H Wu, A unified model for Sierpinski networks with scale-free scaling and small-world effect, *Physica A: Statistical Mechanics and its Applications* **388**, 2571-2578 (2009).
- [46] Z.J Bao, Y.J Cao, L.J Ding, G.Z Wang, Comparison of cascading failures in small-world and scale-free networks subject to vertex and edge attacks, *Physica A: Statistical Mechanics and its Applications* **388**, 4491-4498 (2009).
- [47] X.Y Wang and J.Q Li, Detecting communities by the core-vertex and intimate degree in complex networks, *Physica A: Statistical Mechanics and its Applications* **392**, 2555-2563 (2013).



**Wang Xianchao** received his Ph.D. degree in computer science and technology from School of Computer Engineering and Science of Shanghai University, China, in 2011. He is now an assistant professor and an assistant dean of School of Mathematics and Statistics at the Fuyang Normal College, China. And he is both a member of ACM and a senior of China Computer Federation. His research interests are in applied mathematics including the mathematical methods and models for complex systems, optical computing, complex network, big data and embedded system. He is a reviewer of *Applied Optics* and *Optics Letters*.





**Zuo Kaizhong** received his Ph. D.degree in computer science and technology from the Shanghai University, China, in 2012. He is now a Professor at Anhui Normal University. His research interests include ternary optical computer, ternary polarization hologram

storage, and security and privacy in internet of things. Dr. Zuo is a member of ACM.